energy&fuels

pubs.acs.org/EF Article

Mechanically Stable Thinned Membrane for a High-Performance Polymer Electrolyte Membrane Fuel Cell via a Plasma-Etching and Annealing Process

Tuyet Anh Pham,[§] Le Vu Nam,[§] Eunho Choi, Min-Su Lee, Tea-Sung Jun, Segeun Jang,* and Sang Moon Kim*

Cite This: *Energy Fuels* 2021, 35, 11525−11532 Read Online

ACCESS | Metrics & More | Article Recommendations | Supporting Information

ABSTRACT: A thin electrolyte membrane is highly demanded for achieving high-performance polymer electrolyte membrane fuel cells (PEMFCs) by taking advantage of the reduced ohmic resistance-driven enhanced proton- and water-transport property during the PEMFC operation. However, the thin membrane inherently suffers from poor mechanical properties. In this study, we propose a simple methodological approach that combines the plasma etching and thermal annealing process to construct mechanically stable thinned membrane using commercially available Nafion membranes. The morphological, mechanical, and chemical properties of the modified Nafion membranes were characterized through diverse measurements including field-emission scanning electron microscopy, atomic force microscopy, stress−strain behavior test, and Fourier transform infrared spectrometry. We observed that the plasma etching process effectively reduced the membrane thickness; however, it induced spike-like structures with hundreds of nanometers in size on the membrane surface, which can cause stress-concentration-induced mechanical degradation of the membrane. By adopting a consecutive thermal annealing process, the roughened surface was flattened and mechanical properties including tensile strength and elongation to break were successfully recovered while maintaining the chemical composition of the Nafion. Interestingly, the modified 15 μm-thick Nafion membrane with the plasma etching and thermal process showed a much enhanced maximum power density of 22.5 and 13.6% under the low and high humidity condition of RH 45% @89.5 °C and RH 92% @70 °C, respectively, compared to that of a pristine 25 μm-thick Nafion membrane.

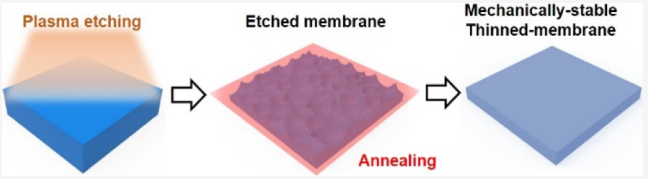

INTRODUCTION

Efficient and environmentally friendly energy systems are in great demand to deal with ever-increasing energy consumption and global decarbonization policies.[1] Among several candidates, fuel cells are considered to be the most promising energy conversion devices for sustainable energy generation due to the direct convertibility of chemical energy into electrical energy with zero emission of pollutants.[2] Especially, the polymer electrolyte membrane fuel cell (PEMFC) using a polymeric material as a proton exchange membrane (PEM) has received great attention for the applications of portable power sources, stationary power generation, and vehicle propulsion[3,4] due to the attractive properties including low operating temperature and high energy conversion efficiency. Although the PEM, as the key component in PEMFCs for ion transport, electric insulation, and barrier for gas crossover, has been extensively studied for decades to achieve low cost, excellent proton-conducting capability, and thermal and mechanical stability,[5] still the perfluorosulfonic acid-based Nafion membrane is dominantly used from the beginning of the PEMFC and it is difficult to find alternatives due to Nafion's inherent electrochemical properties of efficient ion transport in a chemically inert matrix.[6] However, high cost, limited performance, and mechanical/chemical stability of the Nafion membrane are obstacles for further commercialization of the PEMFC.

Until now, many approaches focusing on the improvement of Nafion membrane properties have been attempted to overcome these barriers. First, Nafion composite membranes with blending various metal oxides[7−9] or other polymers[10,11] have been fabricated to sustain high performance at higher operating temperature and pressure.[12] As a physical approach, making a thinned Nafion membrane has been attempted to attain high proton conductivity by applying sand-blasting,[13] ion-bombardment, or plasma etching.[14−16] Interestingly, surface nanoroughness resulted from plasma etching showed an effective role to enlarge the interface area between the electrode and the membrane, where the electrochemical reaction occurs most actively.[14] However, the relationship

Received: April 21, 2021
Revised: May 30, 2021
Published: July 6, 2021

https://doi.org/10.1021/acs.energyfuels.1c01225
Energy Fuels 2021, 35, 11525−11532

Scheme 1. Schematic Illustration of the Consecutive Etching-Annealing Process

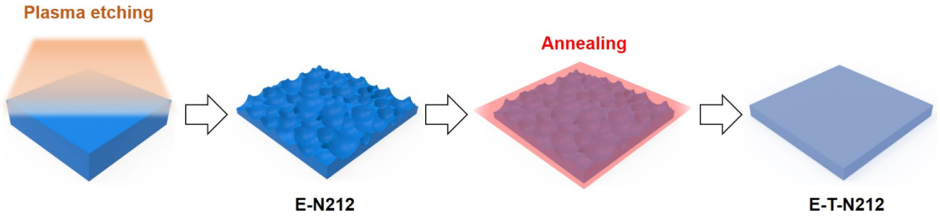

between mechanical properties and morphological changes on the surface should be addressed in more detail since the reduced thickness and high roughness caused by plasma etching can easily induce stress-concentration and crack propagation,[17] which deteriorate the membrane durability. This is because, during the fuel cell operation including the repetitive relative humidity (RH) change cycling, the constrained membrane undergoes swelling-drying-induced internal mechanical stress.[18] In addition, the membrane which has a nonuniform surface with a randomly distributed spike-like structure can easily suffer from locally intensive stress-concentration and result in pinhole and crack formation in the MEA. This mechanical degradation causes lower OCV (open-circuit voltage) because of the increase in the reactant gas crossover across the membrane[17,19] and rapid decline in performance during the RH cycling test.[20] Therefore, it is necessary to improve the mechanical properties of the membrane to secure the long-term operation of the PEMFC. When it comes to thermal annealing during the membrane preparation process, it can alter morphological and mechanical properties of the membrane such as stress−strain behavior,[21,22] ionic conductivity,[23] thermal stability,[24] transport coefficients,[25] and water uptake.[26] Noticeably, this effectiveness of the annealing on the membrane properties depends on many factors such as annealing time, temperature, membrane thickness, and cooling velocity, which means that the annealing condition should be carefully adopted by keeping the proper mechanical property change while minimizing chemical deterioration.

Herein, we propose a simple methodological approach of applying plasma etching followed by an annealing (E-T) process for achieving mechanically stable thinned membrane for high-performance PEMFCs. Although a thinned membrane from plasma etching showed instability during membrane handling or the catalyst deposition process for the construction of membrane electrode assembly (MEA), an additional annealing process made the membrane have much improved mechanical property while maintaining inherent electrochemical properties of the membrane. To elucidate the effect of each of the plasma etching and annealing process, we fabricated and compared diverse membrane samples from the modification of the commercially available Nafion 211 (25 μm) and 212 (50 μm) membrane, which were categorized by pristine Nafion 211/212 (N211/N212), etched N211 (E-N211), thermally treated N211 (T-N211), and etched-thermally treated N211/212 (E-T N211/N212). The changes in morphology and physicochemical property through the membrane modification process were characterized by stress−strain curves, field-emission scanning electron microscopy (FE-SEM), atomic force microscopy (AFM), Fourier transform infrared spectrometry (FT-IR), and thermogravimetric analysis (TGA). Besides, the electrochemical properties from single-cell tests were confirmed through the measurements of electrochemical impedance spectroscopy (EIS) and cyclic voltammograms (CVs). Interestingly, the E-T-N212 exhibited greater mechanical properties and slightly higher performance compared to the N211 with the same thickness (~25 μm). Remarkably, E-T-N211, which had the thinnest thickness of ~15 μm, showed significantly improved PEFMC performances under diverse operating conditions while maintaining sufficient mechanical properties due to enhanced proton/water transportation from the membrane-thinning effect and thermal annealing effect.

EXPERIMENTAL SECTION

Membrane Preparation. N212 (thickness: ~50 μm) and N211 (thickness: ~25 μm) (DuPont, USA) were etched to 25 and 15 μm, respectively, using plasma etching. The process was carried out with a radio frequency power of 100 W and a flow rate of 20 sccm with supplying air to the chamber by keeping the pressure of 0.12 Torr. The etch rate of the process was determined by measuring the etch depth with a variation of etching time. Consequently, the operating time to obtain a membrane thickness of 25 μm for N212 and 15 μm for N211 was 2.5 and 1 h, respectively (Figure S1). After plasma modification, etched membranes (E-N212 and E-N211) were annealed on the glass substrate at 200 °C for 2 h. Accordingly, the thermally treated membranes were designated as E-T-N212 and E-T-N211. Scheme 1 schematically illustrates the preparation procedure of the modified membranes. To verify the effect of the solely annealing or etching process compared to the consecutive etching-annealing process on the performance of the membrane, we fabricated a thermally annealed N211 membrane without plasma etching (T-N211) and an etched N211 membrane without thermal annealing (E-N211). Finally, pristine N211/N212, E-N211, T-N211, and E-T N211/N212 were prepared to compare the membrane properties.

Physical Analysis. Surface morphology of the membranes after each step in the process was observed using FE-SEM (Carl Zeiss, Germany) operated at 20 kV and AFM (Bruker, USA). FT-IR (Bruker, USA) spectra were recorded in the range of 4000−500 cm^{-1} in the transmittance mode to analyze the chemical structure of the Nafion membrane before and after the etching-annealing treatment. The tensile responses of the conventional and modified membranes were prepared with the identical sample size (10 mm width and 20 mm length) and measured at room temperature using a stretching machine (Instron Corp, USA) with a strain rate of 5 mm/min.

MEA Fabrication. The catalyst-coated membrane (CCM) for the MEAs with an active area of 5 cm^2 was fabricated by a direct spray-coating method with catalyst ink. The ink was prepared by mixing Pt/C 40 wt % (Johnson Matthey, USA) with a solvent consisting of deionized water, isopropyl alcohol (Sigma-Aldrich, USA), and Nafion solution 5 wt % (DuPont, USA) and further treated with ultrasonication for 20 min. The platinum loading was fixed at 0.2 mg/cm^2 on both anode and cathode sides. Afterward, the prepared MEA was placed between two gas diffusion layers (35BC, SGL Carbon, Germany), two Teflon gaskets, and two serpentine gas flow channels (width: ~1 mm). The prepared single-cell assembly was tightly fastened by eight bolts with a torque of 70 ft-lb.

Single-Cell Testing and Electrochemical Characterization. For electrochemical polarization tests, the single cell was connected to a PEMFC test system (CNL Energy, Korea) by supplying humidified

https://doi.org/10.1021/acs.energyfuels.1c01225
Energy Fuels 2021, 35, 11525−11532

H_2 (300 mL/min) and air (1000 mL/min) to the anode and cathode, respectively. Moreover, two operating conditions (RH 92% @70 °C and RH 45% @89.5 °C) were utilized for evaluating each MEA performance. Then, EIS measurements were conducted under the same conditions as polarization tests. EIS spectra (HCP 803, Biologic, France) were measured at 0.5 V with an amplitude of 5 mV in the range of frequency from 0.1 Hz to 100 kHz. To evaluate the electrochemical active surface (ECSA) of the cathode electrode, CVs were conducted at 70 °C with supplying fully humidified N_2 (200 mL/min) and H_2 (200 mL/min) to the cathode (working electrode) and anode (the counter and reference electrode), respectively. The voltage of the working electrode was swept at a scan rate of 100 mV/s between 0.05 and 1.20 V.

RESULTS AND DISCUSSION

Mechanical Properties of E-T-N212 and E-T-N211. Scheme 1 shows a schematical illustration of the consecutive plasma etching and annealing process for obtaining the modified membranes. First, the plasma etching process was conducted to the pristine Nafion membrane attached on the glass substrate. During the process, the ionized gas bombardment induced the decomposition of the polymeric chain, which reduced the membrane thickness and increased the surface roughness of the membrane. Then, the following annealing process at over the glass transition temperature of the Nafion membrane flattened the etched membrane surface by inducing the viscoelastic behavior of the polymer. Figure 1 displays the surface morphology of the modified membranes after the plasma etching and annealing process observed by SEM and AFM. The surface of pristine N211 with a thickness of ~25 μm (Figure 1a) was found to be distinctly smooth. Nonetheless, the surface of E-N212 with a thickness of ~25 μm was irregular and rugged, as seen in Figure 1b, which indicated that plasma treatment not only decreased membrane thickness but also modified the surface topography. Specifically, we observed that the root-mean-square (RMS) factor, which reflects the extent of surface roughness, increased dramatically from 1.61 to 331 nm and this is consistent with the previous plasma etching studies.[14−16,27,28] To investigate the surface morphology change depending on the annealing temperature, we have varied annealing temperatures. It has been reported that the Nafion membrane has two kinds of glass transition temperatures (T_g). The first T_g, which causes rearrangement of the main chain, ranges from 100 to 130 °C[29,30] while the second T_g, which causes reconfiguration of the side chain, is approximately 240 °C.[31] In our experiments, the annealing temperature was chosen between these two T_g ranges to obtain a flattening effect without deterioration of proton conductivity of the membrane. Furthermore, as presented in the previous studies of TGA measurement of the Nafion membrane, the breakup of the H_3O^+ in the hydrated ionic group of $SO_3(H_3O)$ to SO_3H, as well as partial decomposition of SO_3H to SO_2 and $^{\bullet}OH$, occurs over 200 °C,[6,32] which can reduce proton conductivity of the membrane. Therefore, we set the annealing temperature in the range from 100 to 200 °C and carried out annealing experiments at the temperatures of 100 °C (E-T100-N212), 130 °C (E-T130-N212), 160 °C (E-T160-N212), and 200 °C (E-T200-N212). To confirm the surface morphology change in the membrane after annealing at a different temperature, SEM measurement was conducted, as shown in Figure S2. Roughness on the surface caused by plasma etching was gradually reduced with increasing annealing temperature. Noticeably, the surface of the membrane with 200 °C annealing temperature was nearly flat. To check if the spike-like structure on the surface affects the mechanical properties of the membrane due to crack propagation, stress−strain responses of etched-annealed Nafion membranes were recorded, as shown in Figure S3. As the annealing temperature increased, mechanical properties, including tensile strength and elongation to break, were enhanced. Noticeably, E-T200-N212 exhibited higher mechanical properties than other membranes with different annealing temperatures. This result indicates that the mechanical strength of the membrane gets increased as the extent of the randomly distributed spike-like structure gets alleviated. As a result, annealing temperature at 200 °C was used in this paper to alleviate the surface roughness and improve mechanical properties. Through the consecutive annealing process at 200 °C, the RMS value was dramatically reduced to 21.3 nm, and the spike-like structure on the surface of the etched membrane was completely removed (Figure 1c). A similar trend was also observed with thinner membranes, E-N211 and E-T-N211. As shown in Figure 1d, E-N211 had a rugged surface with a mean thickness of about 15 μm. After annealing, the RMS reduced significantly from 314 to 21.3 nm, which was a nearly flat surface (Figure 1e). The mean thickness of the membranes is summarized in Table 1. Next, to

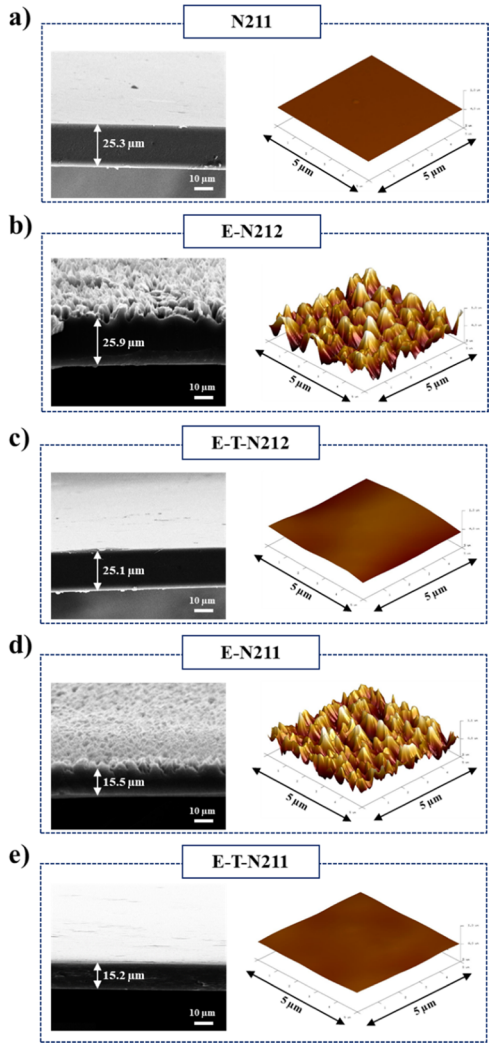

Figure 1. Surface morphology examined by SEM (left) and AFM (right) of (a) N211, (b) E-N211, (c) E-T-212, (d) E-N211, and (e) E-T-N211 membranes.

https://doi.org/10.1021/acs.energyfuels.1c01225
Energy Fuels 2021, 35, 11525−11532

Table 1. Thickness of Modified Membranes and Conventional Membranes

membrane	mean thickness	maximum thickness	minimum thickness
N212	50	51	49
N211	25	26	25
E-N211	15	17	13
T-N211	25	26	25
E-T-N212	25	25	24
E-T-N211	15	16	14

investigate the changes in chemical properties of the modified membrane by the E-T process, FT-IR spectra in the range of 500−4000 cm^{-1} were obtained along with the vibrational bands assigning the presence of the corresponding functional group (Figure 2 and Table 2). The chemical species in the E-T-N212 membrane were maintained without deterioration during the etching and thermal annealing process thanks to the high thermal stability of the Nafion material which has a PTFE-like molecular backbone. This result is in good agreement with TGA in previous papers.[33−35] The chemical structure of the Nafion membrane remains under 300 °C except for the loss of (residual) water, and thermal decomposition of Nafion occurs from 300 °C through the cleavage of distinct groups.[32,36] Accordingly, it can be seen that the E-T process changed the physical properties (thickness, surface roughness, etc.) of the Nafion membrane without affecting the chemical composition.

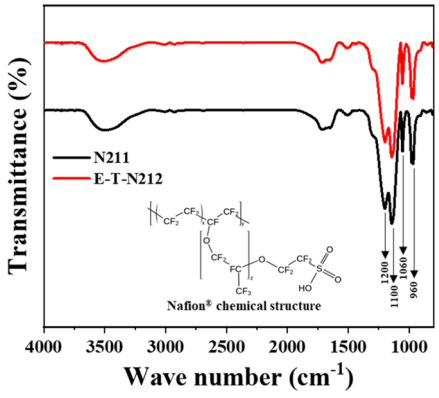

Figure 2. FTIR spectra of N211 and E-T-N212 membranes.

Table 2. Selected Infrared Absorption Bands of Nafion

band Location (cm^{-1})	assignment
1200	CF2 stretching, asymmetric
1100	CF2 stretching, symmetric
1060	S−O stretching, symmetric
960	C−O−C stretching, symmetric

To evaluate the mechanical properties including Young's modulus, ultimate tensile stress, and elongation to break of the modified membranes, uniaxial tensile strength tests for each membrane were conducted. Figure 3a presents the stress−strain curves for the membranes with a thickness of ∼15 μm (E-N211 and E-T-N211), ∼25 μm (N211, T-N211, and E-T-N212), and ∼50 μm (N212). The measured values of tensile strength, elongation to break, and Young's modulus of these membranes are shown in Figure 3b−d, respectively. It is noticeable that the E-N211 membrane, with random nano-textures on the surface and thinnest thickness caused by plasma etching, showed extremely low Young's modulus, tensile strength, and elongation to break. Specifically, the tensile strength of the E-N211 membrane was about 77 and 74% lower than the pristine N212 and N211 membranes, respectively. This result may come from the fact that the crack initiation and propagation were facilitated by the randomly distributed nanoroughness on the thinned membrane during the stretching process. Also, this can limit the lifetime of the membrane and also cause the increase in the reactant gas crossover across the membrane which leads to radical formation-induced chemical degradation of the membrane and generation of mixed potential.[19,37] Meanwhile, after the annealing process, the stress−strain curve of the membranes (T-N211, E-T-N212, and E-T-N211) revealed significantly improved mechanical properties compared to pristine Nafion membranes and the etched membrane without thermal annealing. Noticeably, as illustrated in Figure 3c,d, the tensile strength and the elongation to break of the thinned E-T-N211 membrane were very much higher than those of the E-N211 membrane with the same thickness (∼15 μm). Indeed, since the E-N211 was easily damaged during detaching from the substrate or spraying catalyst onto the surface due to the thinned thickness with high roughness (Figure S4), the annealing process is essential for the membrane with thickness under 15 μm to prevent this disruption. Furthermore, other thermally treated membranes (E-T-N212 and T-N211) showed a comparable trend in the stress−strain curve with increased tensile stress than N211 with the same thickness (∼25 μm). Accordingly, the additional annealing process in this study plays an effective role in enhancing mechanical properties of the membrane because heat treatment can induce higher crystallinity in the polymer matrix, leading to stronger molecular bonding between the polymer chains.[38−40] Moreover, it can mitigate crack initiation and propagation by flattening the etched surface roughness. Additionally, the thermal decomposition property of the membranes was analyzed through TGA. Generally, the Nafion membrane undergoes three weight-loss stages. (1) At a temperature under 200 °C, the membrane loses weight due to the loss of water bonded to the sulfonic group. (2) In the second stage (280 ± 30 to 400 ± 20 °C), the cleavage of the C−S bond from the degradation of the side chain sulfonic acid group occurs. (3) At the final stage (400 ± 20 to 600 ± 40 °C), decomposition of the polymer main chain results in over 90% volatilization of the membrane component.[40−43] As shown in Figure S5, TGA curves of T-N211 exhibited a delayed weight loss until the final stage, which implies that the annealing process can strengthen interactions among polymer chains in the membrane and therefore increases the thermal stability of the membrane.[24] Therefore, a mechanically stable thinned membrane for high-performance fuel cells with durability can be achieved using the E-T process.

Effect of the E-T Process on MEA Performance. To investigate the effect of the E-T procedure on the PEMFC performance, we conducted the performance measurements of MEAs with E-T-N212, E-T-N211, T-N211, and N211 under the nearly fully humidified and low RH conditions (Figure 4 and Table 3). Figure 4a shows the polarization curves of prepared MEAs under the RH 92% @70 °C condition. Under this condition, the MEA with pristine N211 exhibited the lowest power density of 0.778 W/cm^2 while the modified membranes with the same thickness (∼25 μm) showed a

https://doi.org/10.1021/acs.energyfuels.1c01225
Energy Fuels 2021, 35, 11525−11532

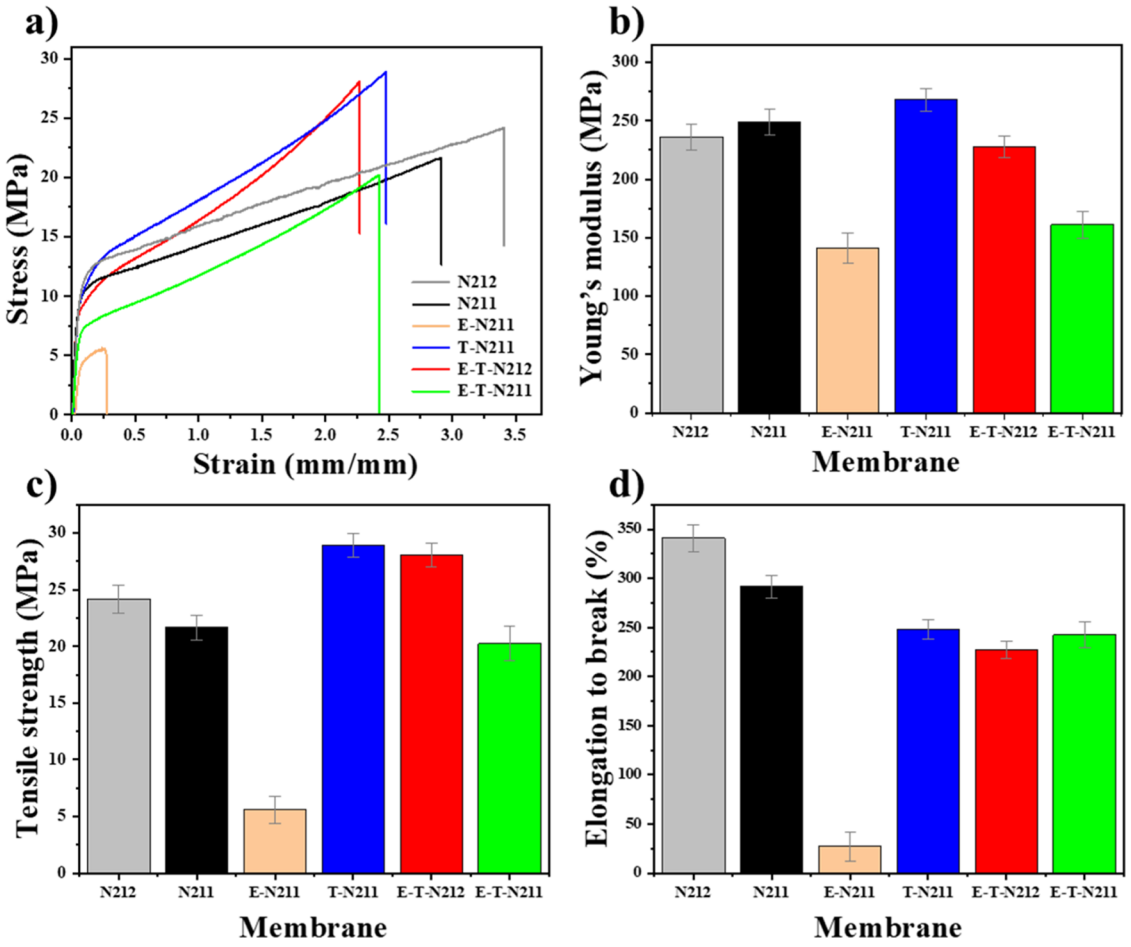

Figure 3. Mechanical properties of the membranes: (a) stress−strain curves, (b) Young's modulus, (c) tensile strength, and (d) elongation to break.

slightly enhanced performance of 0.789 W/cm^2 (T-N211) and 0.802 W/cm^2 (E-T-N212). This means that the thermal annealing and etching process does not deteriorate the electrochemical properties of the pristine membrane, and rather, the thermal annealing process may improve the MEA performance with normalizing the transport properties from the flattening effect and reorganization of the structure above the glass transition temperature of the Nafion.[21,23,25] When it comes to the E-T-N211 membrane (~15 μm), it showed a much-increased maximum power density of 0.884 W/cm^2, which is 13.6% higher than that of pristine N211. This mainly came from the thickness reduction (~40%) effect-driven improved proton conductivity (i.e., decreased ohmic resistance) and enhanced water management (water back diffusion from the shortened pathway). To further assess the membrane-thinning effect of the E-T-N211 membrane for PEMFC performance, we compared polarization curves of each MEA at RH 45% @89.5 °C. Generally known, under the high temperature and low RH operating condition of PEMFC, the water content in the membrane and ionomer network in the electrode is reduced, which induces reduced proton conductivity and electrode reaction kinetics.[44−46] In addition, the performance degradation due to the low RH operating condition can be alleviated using a thinned membrane, which enhances the water back diffusion and results in balancing water content in the MEA. In our experiment, to decrease the RH condition while maintaining water bath temperature at ~70 °C, the cell operating temperature was increased to 89.5 °C. Under this operating condition, the decreased proton conductivity from dehydration of the membrane and the electrode is responsible for the noticeable reduction in the maximum performance of the MEAs. Particularly, as presented in Figure 4b, the power density of the pristine N211 rapidly decreased about 46.9% from 0.778 to 0.413 W/cm^2 under the low RH condition. However, the MEA with E-T-N211 exhibited a much higher performance about 0.506 W/cm^2 which was 22.5% larger than that of the MEA with pristine N211. This implies that the etching process followed by the annealing process has a substantial effect on the performance enhancement of the PEMFC by reducing the membrane thickness while attaining proper mechanical property. In addition, based on the fact that the thinned membrane, E-T-211, shows performance improvement of 13.6% under the high RH condition and 21.3% under the low RH condition compared to N211, as shown in Table 3. The results indicate that the membrane-thinning effect on the performance improvement becomes greater as the RH gets decreased.

To elucidate the electrochemical properties of the MEAs with the modified membranes through the E-T process, EIS and CV measurements were carried out. The EIS spectra at 0.5 V were measured and are plotted in Figure 5a−b. The EIS measuring condition was set to correspond to the operating condition of the polarization test under RH 92% @70 °C and RH 45% @89.5 °C. The ohmic resistance (R_Ω) and the kinetic

https://doi.org/10.1021/acs.energyfuels.1c01225
Energy Fuels 2021, 35, 11525−11532

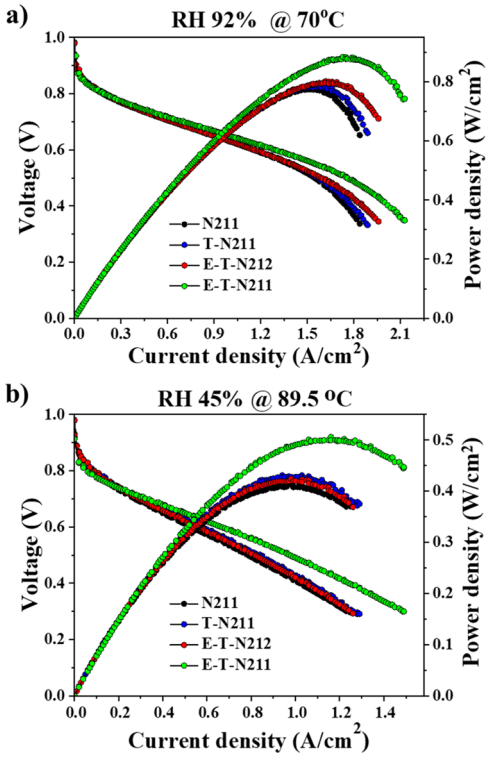

Figure 4. Polarization curves of MEAs with N211, T-N211, E-T-N212, and E-T-N211 membranes: (a) RH 92% @70 °C and (b) RH 45% @89.5 °C.

Table 3. Maximum Power Density of the MEAs with N211, T-N211, E-T-N212, and E-T-N211 Membranes

membrane	max. power density (W/cm^2) RH 92%@70 °C	max. power density (W/cm^2) RH 45%@89.5 °C
N211	0.778 (100.0%)	0.413 (100.0%)
T-N211	0.789 (101.4%)	0.431 (104.4%)
E-T-N212	0.802 (103.1%)	0.424 (102.7%)
E-T-N211	0.884 (113.6%)	0.501 (121.3%)

resistance (R_C) calculated from EIS spectra are presented in Table 4 with the corresponding equivalent circuit (Figure S6). Under a high humidity condition of RH 92% @70 °C, there were significant reductions in both R_Ω (0.0455 Ω cm^2) and R_C (0.3283 Ω cm^2) of the MEA with E-T-N211 compared to those of the MEA with pristine N211 (R_Ω = 0.0576 and R_C = 0.4326 Ω cm^2) due to reduced membrane thickness-induced improved proton conductivity and enhanced water management at high current density from the shortened water back diffusion pathway. In the case of the low RH operating condition, as illustrated in Figure 5b, the noticeable difference was observed in R_Ω (0.0844 Ω cm^2) of the MEA with E-T-N211 compared to the that of the MEA with pristine N211 (0.1324 Ω cm^2), which means that the thinned membrane can effectively attain much water from the enhanced water back diffusion from the cathode to anode. After analysis of the $I-V$ performance of each MEA, the ECSA of each sample was obtained from CV measurements (Figure 5c). As shown in Table 4, all prepared samples exhibited comparable ECSA values of 56.864 m^2/g (N211), 55.751 m^2/g (T-N211), 55.385 m^2/g (E-T-N212), and 56.612 m^2/g (E-T-N211), which indicate that the E-T process did not affect the morphology or distribution of the catalyst layer and all the MEAs were made

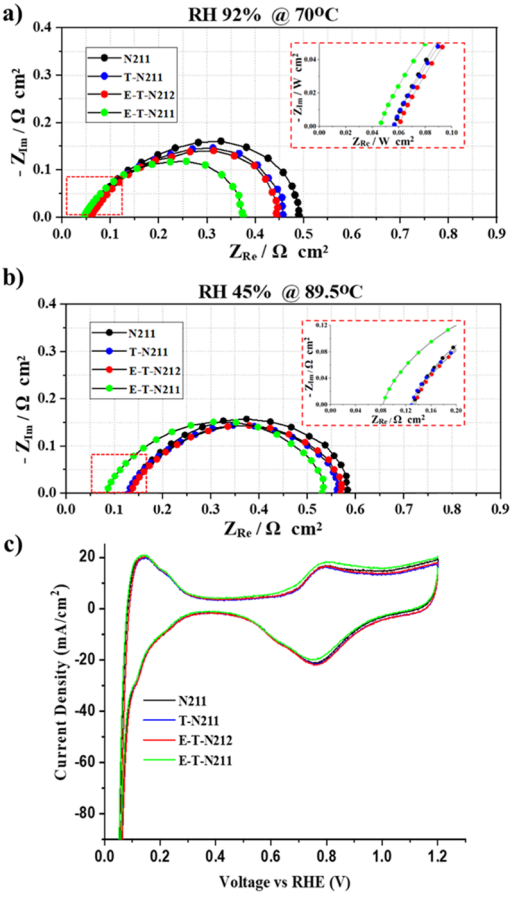

Figure 5. EIS measurements at 0.5 V of N211, T-N211, E-T-N212, and E-T-N211 membranes at (a) RH 92% @70 °C and (b) RH 45% @89.5 °C and (c) CV measurements of MEA of N211, T-N211, E-T-N212, and E-T-N211 membranes.

Table 4. Electrochemical Characterizations of N211, T-N211, E-T-N212, and E-T-N211 MEAs

	RH 92%@70 °C		RH 45%@89.5 °C		
membrane	R_Ω at 0.5 V (Ω cm^2)	R_C at 0.5 V (Ω cm^2)	R_Ω at 0.5 V (Ω cm^2)	R_C at 0.5 V (Ω cm^2)	ECSA (m^2/g)
N211	0.0576	0.4326	0.1324	0.4492	56.864
T-N211	0.0559	0.4008	0.1307	0.4293	55.751
E-T-N212	0.0602	0.3841	0.1361	0.4301	55.385
E-T-N211	0.0455	0.3283	0.0844	0.4433	56.612

with the same amount of catalyst. Finally, to check the morphology of each catalyst layer, the constructed MEAs with the membranes of N211, T-N211, E-T-N212, and E-T-N211 were observed by cross-sectional SEM images, as shown in Figure S7. As expected, each MEA had a similar electrode thickness of ~6 μm and the electrodes were uniformly deposited on the membrane surface. Besides, unlike other MEAs with a membrane thickness of ~25 μm, we observed that the MEA with E-T-N211 showed significantly reduced MEA thickness due to the thinned membrane.

CONCLUSIONS

In this study, we achieved a high-performance fuel cell with a mechanically stable, thinned Nafion membrane by the consecutive plasma etching and annealing process. It was

https://doi.org/10.1021/acs.energyfuels.1c01225
Energy Fuels 2021, 35, 11525−11532

confirmed that the plasma etching process effectively reduced thickness and changed the surface morphology of the membrane. However, spike-like structures with hundreds of nanometers in size on the surface from plasma etching induced mechanical failure during the tensile stress test due to stress-concentration effect and crack propagation. By applying the successive thermal annealing process, the rugged-surface morphology was successfully flattened and mechanical properties including tensile strength and elongation to break were recovered while maintaining the chemical composition of the Nafion. When it comes to PEMFC performance, the MEA with E-T-N211 (15 μm) showed a remarkably improved maximum power density, which was 13.6 and 22.52% higher than those of the MEA with pristine N211 under the operating condition of RH 92% @70 °C and RH 45% @89.5 °C. It is conjectured that the thinned membrane induced reduction in the ohmic resistance and enhancement of the water management by a shortened water back diffusion pathway. Therefore, the E-T process is suitable to be used to reduce membrane thickness and improve the PEMFC performance under diverse operating conditions while maintaining the sufficient mechanical properties of the membrane.

■ ASSOCIATED CONTENT

Supporting Information

The Supporting Information is available free of charge at https://pubs.acs.org/doi/10.1021/acs.energyfuels.1c01225.

Plasma etch rate; SEM images for etched membranes and MEAs; strain−stress curve of the annealed membrane; TGA; and equivalent circuit of the PEMFC (PDF)

■ AUTHOR INFORMATION

Corresponding Authors

Segeun Jang − *School of Mechanical Engineering, Kookmin University, Seoul 02707, Republic of Korea*; Email: sjang@kookmin.ac.kr

Sang Moon Kim − *Department of Mechanical Engineering, Incheon National University, Incheon 22012, Republic of Korea*; orcid.org/0000-0002-2311-2211; Email: ksm7852@inu.ac.kr

Authors

Tuyet Anh Pham − *Department of Mechanical Engineering, Incheon National University, Incheon 22012, Republic of Korea*

Le Vu Nam − *Department of Mechanical Engineering, Incheon National University, Incheon 22012, Republic of Korea*

Eunho Choi − *School of Mechanical Engineering, Kookmin University, Seoul 02707, Republic of Korea*

Min-Su Lee − *Department of Mechanical Engineering, Incheon National University, Incheon 22012, Republic of Korea*

Tea-Sung Jun − *Department of Mechanical Engineering, Incheon National University, Incheon 22012, Republic of Korea*

Complete contact information is available at: https://pubs.acs.org/10.1021/acs.energyfuels.1c01225

Author Contributions

[§]T.A.P. and L.V.N. contributed equally to this work.

Notes

The authors declare no competing financial interest.

■ ACKNOWLEDGMENTS

This research was supported by the Korea Electric Power Corporation (grant number: R19XO01-29) and the National Research Foundation (NRF) of Korea (grant no. 2019R1C1C1004462).

■ ABBREVIATIONS

PEMFC = polymer electrolyte membrane fuel cell
PEM = proton exchange membrane
MEA = membrane-electrode assembly
FE-SEM = field-emission scanning electron microscopy
AFM = atomic force microscopy
FT-IR = Fourier transform infrared spectrometry
EIS = electrochemical impedance spectroscopy
CVs = cyclic voltammograms
CCM = catalyst-coated membrane
RH = relative humidity
ECSA = electrochemical surface area

■ REFERENCES

(1) Kirubakaran, A.; Jain, S.; Nema, R. K. A Review on Fuel Cell Technologies and Power Electronic Interface. *Renew. Sustain. Energy Rev.* **2009**, *13*, 2430−2440.

(2) Hirschenhofer, J. H.; Stauffer, D. B.; Engleman, R. R.; Klett, M. G. *Fuel Cell Handbook*; Federal Energy Technology Center, 1998.

(3) Ajanovic, A.; Haas, R. Economic Prospects and Policy Framework for Hydrogen as Fuel in the Transport Sector. *Energy Pol.* **2018**, *123*, 280−288.

(4) Hames, Y.; Kaya, K.; Baltacioglu, E.; Turksoy, A. Analysis of the Control Strategies for Fuel Saving in the Hydrogen Fuel Cell Vehicles. *Int. J. Hydrogen Energy* **2018**, *43*, 10810−10821.

(5) Sigwadi, R.; Dhlamini, M. S.; Mokrani, T.; Nemavhola, F.; Nonjola, P. F.; Msomi, P. F. The proton conductivity and mechanical properties of Nafion/ ZrP nanocomposite membrane. *Heliyon* **2019**, *5*, No. e02240.

(6) Kusoglu, A.; Weber, A. Z. New Insights into Perfluorinated Sulfonic-Acid Ionomers. *Chem. Rev.* **2017**, *117*, 987−1104.

(7) Di Noto, V.; Lavina, S.; Negro, E.; Vittadello, M.; Conti, F.; Piga, M.; Pace, G. Hybrid Inorganic-Organic Proton Conducting Membranes Based on Nafion and 5 Wt% of MxOy (M = Ti, Zr, Hf, Ta and W). Part II: Relaxation Phenomena and Conductivity Mechanism. *J. Power Sources* **2009**, *187*, 57−66.

(8) Saccà, A.; Carbone, A.; Gatto, I.; Pedicini, R.; Freni, A.; Patti, A.; Passalacqua, E. Composites Nafion-Titania Membranes for Polymer Electrolyte Fuel Cell (PEFC) Applications at Low Relative Humidity Levels: Chemical Physical Properties and Electrochemical Performance. *Polym. Test.* **2016**, *56*, 10−18.

(9) Gagliardi, G. G.; Ibrahim, A.; Borello, D.; El-Kharouf, A. Composite Polymers Development and Application for Polymer Electrolyte Membrane Technologies-a Review. *Molecules* **2020**, *25*, 1712−7256.

(10) Zhang, B.; Cao, Y.; Jiang, S.; Li, Z.; He, G.; Wu, H. Enhanced Proton Conductivity of Nafion Nanohybrid Membrane Incorporated with Phosphonic Acid Functionalized Graphene Oxide at Elevated Temperature and Low Humidity. *J. Membr. Sci.* **2016**, *518*, 243−253.

(11) Dai, Y.; Wang, J.; Tao, P.; He, R. Various Hydrophilic Carbon Dots Doped High Temperature Proton Exchange Composite Membranes Based on Polyvinylpyrrolidone and Polyethersulfone. *J. Colloid Interface Sci.* **2019**, *553*, 503−511.

(12) Schalenbach, M.; Stolten, D. High-Pressure Water Electrolysis: Electrochemical Mitigation of Product Gas Crossover. *Electrochim. Acta* **2015**, *156*, 321−327.

(13) Wang, Y.; Zhu, Z.; Liu, J.; Chang, L.; Chen, H. Effects of Surface Roughening of Nafion 117 on the Mechanical and Physicochemical Properties of Ionic Polymer-Metal Composite (IPMC) Actuators. *Smart Mater. Struct.* **2016**, *25*, 085012.

(14) Van Nguyen, T.; Vu Nguyen, M.; Nordheden, K. J.; He, W. Effect of Bulk and Surface Treatments on the Surface Ionic Activity of Nafion Membranes. *J. Electrochem. Soc.* **2007**, *154*, A1073−A1076.
(15) Cho, Y.-H.; Bae, J. W.; Cho, Y.-H.; Lim, J. W.; Ahn, M.; Yoon, W.-S.; Kwon, N.-H.; Jho, J. Y.; Sung, Y.-E. Performance Enhancement of Membrane Electrode Assemblies with Plasma Etched Polymer Electrolyte Membrane in PEM Fuel Cell. *Int. J. Hydrogen Energy* **2010**, *35*, 10452−10456.
(16) Omosebi, A.; Besser, R. S. Ultra-low Mass Sputtered and Conventional Catalyst Layers on Plasma-etched Nafion for PEMFC Applications. *Fuel Cells* **2017**, *17*, 762−769.
(17) Zhang, Z.; Shi, S.; Lin, Q.; Wang, L.; Liu, Z.; Li, P.; Chen, X. Exploring the Role of Reinforcement in Controlling Fatigue Crack Propagation Behavior of Perfluorosulfonic-Acid Membranes. *Int. J. Hydrogen Energy* **2018**, *43*, 6379−6389.
(18) Huang, X.; Solasi, R.; Zou, Y.; Feshler, M.; Reifsnider, K.; Condit, D.; Burlatsky, S.; Madden, T. Mechanical Endurance of Polymer Electrolyte Membrane and PEM Fuel Cell Durability. *J. Polym. Sci., Part B: Polym. Phys.* **2006**, *44*, 2346−2357.
(19) Rodgers, M. P.; Bonville, L. J.; Kunz, H. R.; Slattery, D. K.; Fenton, J. M. Fuel Cell Perfluorinated Sulfonic Acid Membrane Degradation Correlating Accelerated Stress Testing and Lifetime. *Chem. Rev.* **2012**, *112*, 6075−6103.
(20) Vengatesan, S.; Fowler, M. W.; Yuan, X.-Z.; Wang, H. Diagnosis of MEA Degradation under Accelerated Relative Humidity Cycling. *J. Power Sources* **2011**, *196*, 5045−5052.
(21) Li, J.; Yang, X.; Tang, H.; Pan, M. Durable and High Performance Nafion Membrane Prepared through High-Temperature Annealing Methodology. *J. Membr. Sci.* **2010**, *361*, 38−42.
(22) Maldonado, L.; Perrin, J.-C.; Dillet, J.; Lottin, O. Characterization of Polymer Electrolyte Nafion Membranes: Influence of Temperature, Heat Treatment and Drying Protocol on Sorption and Transport Properties. *J. Membr. Sci.* **2012**, *389*, 43−56.
(23) Kwon, O.; Wu, S.; Zhu, D.-M. Configuration Changes of Conducting Channel Network in Nafion Membranes Due to Thermal Annealing. *J. Phys. Chem. B* **2010**, *114*, 14989−14994.
(24) Feng, K.; Hou, L.; Tang, B.; Wu, P. Does Thermal Treatment Merely Make a H2O-Saturated Nafion Membrane Lose Its Absorbed Water at High Temperature? *Phys. Chem. Chem. Phys.* **2015**, *17*, 9106−9115.
(25) Hensley, J. E.; Way, J. D.; Dec, S. F.; Abney, K. D. The Effects of Thermal Annealing on Commercial Nafion Membranes. *J. Membr. Sci.* **2007**, *298*, 190−201.
(26) Evans, C. E.; Noble, R. D.; Nazeri-Thompson, S.; Nazeri, B.; Koval, C. A. Role of Conditioning on Water Uptake and Hydraulic Permeability of Nafion Membranes. *J. Membr. Sci.* **2006**, *279*, 521−528.
(27) Taylor, E. P.; Landis, F. A.; Page, K. A.; Moore, R. B. Counterion Dependent Crystallization Kinetics in Blends of a Perfluorosulfonate Ionomer with Poly(Vinylidene Fluoride). *Polymer (Guildf).* **2006**, *47*, 7425−7435.
(28) Ha, J.-W.; Park, S. Micro-Porous Patterning of the Surface of a Polymer Electrolyte Membrane by an Accelerated Plasma and Its Performance for Direct Methanol Fuel Cells. *Macromol. Res.* **2017**, *25*, 1−4.
(29) Jung, H.-Y.; Kim, J. W. Role of the Glass Transition Temperature of Nafion 117 Membrane in the Preparation of the Membrane Electrode Assembly in a Direct Methanol Fuel Cell (DMFC). *Int. J. Hydrogen Energy* **2012**, *37*, 12580−12585.
(30) Mohamed, H. F. M.; Kobayashi, Y.; Kuroda, C. S.; Ohira, A. Effects of Ion Exchange on the Free Volume and Oxygen Permeation in Nafion for Fuel Cells. *J. Phys. Chem. B* **2009**, *113*, 2247−2252.
(31) Corti, H. R.; Nores-Pondal, F.; Pilar Buera, M. Low Temperature Thermal Properties of Nafion 117 Membranes in Water and Methanol-Water Mixtures. *J. Power Sources* **2006**, *161*, 799−805.
(32) Iwai, Y.; Yamanishi, T. Thermal Stability of Ion-Exchange Nafion N117CS Membranes. *Polym. Degrad. Stab.* **2009**, *94*, 679−687.
(33) Samms, S. R.; Wasmus, S.; Savinell, R. F. Thermal Stability of Nafion in Simulated Fuel Cell Environments. *J. Electrochem. Soc.* **1996**, *143*, 1498−1504.
(34) Liang, Z.; Chen, W.; Liu, J.; Wang, S.; Zhou, Z.; Li, W.; Sun, G.; Xin, Q. FT-IR Study of the Microstructure of Nafion Membrane. *J. Membr. Sci.* **2004**, *233*, 39−44.
(35) Omosebi, A.; Besser, R. S. Electron Beam Patterned Nafion Membranes for DMFC Applications. *J. Power Sources* **2013**, *228*, 151−158.
(36) Feng, M.; Qu, R.; Wei, Z.; Wang, L.; Sun, P.; Wang, Z. Characterization of the Thermolysis Products of Nafion Membrane: A Potential Source of Perfluorinated Compounds in the Environment. *Sci. Rep.* **2015**, *5*, 9859.
(37) Baik, K. D.; Hong, B. K.; Kim, M. S. Novel Technique for Measuring Oxygen Crossover through the Membrane in Polymer Electrolyte Membrane Fuel Cells. *Int. J. Hydrogen Energy* **2013**, *38*, 8927−8933.
(38) Alberti, G.; Narducci, R.; Sganappa, M. Effects of Hydrothermal/Thermal Treatments on the Water-Uptake of Nafion Membranes and Relations with Changes of Conformation, Counter-Elastic Force and Tensile Modulus of the Matrix. *J. Power Sources* **2008**, *178*, 575−583.
(39) Kusoglu, A.; Savagatrup, S.; Clark, K. T.; Weber, A. Z. Role of Mechanical Factors in Controlling the Structure-Function Relationship of PFSA Ionomers. *Macromolecules* **2012**, *45*, 7467−7476.
(40) Yin, C.; Wang, Z.; Luo, Y.; Li, J.; Zhou, Y.; Zhang, X.; Zhang, H.; Fang, P.; He, C. Thermal Annealing on Free Volumes, Crystallinity and Proton Conductivity of Nafion Membranes. *J. Phys. Chem. Solids* **2018**, *120*, 71−78.
(41) Teng, X.; Dai, J.; Su, J.; Yin, G. Modification of Nafion Membrane Using Fluorocarbon Surfactant for All Vanadium Redox Flow Battery. *J. Membr. Sci.* **2015**, *476*, 20−29.
(42) Morita, S.; Kitagawa, K. Temperature-Dependent Structure Changes in Nafion Ionomer Studied by PCMW2D IR Correlation Spectroscopy. *J. Mol. Struct.* **2010**, *974*, 56−59.
(43) Lage, L. G.; Delgado, P. G.; Kawano, Y. Thermal stability and decomposition of nafion membranes with different cations. *J. Therm. Anal. Calorim.* **2004**, *75*, 521−530.
(44) Knights, S. D.; Colbow, K. M.; St-Pierre, J.; Wilkinson, D. P. Aging Mechanisms and Lifetime of PEFC and DMFC. *J. Power Sources* **2004**, *127*, 127−134.
(45) Zhang, J.; Tang, Y.; Song, C.; Xia, Z.; Li, H.; Wang, H.; Zhang, J. PEM Fuel Cell Relative Humidity (RH) and Its Effect on Performance at High Temperatures. *Electrochim. Acta* **2008**, *53*, 5315−5321.
(46) Jeon, D. H.; Kim, K. N.; Baek, S. M.; Nam, J. H. The Effect of Relative Humidity of the Cathode on the Performance and the Uniformity of PEM Fuel Cells. *Int. J. Hydrogen Energy* **2011**, *36*, 12499−12511.

https://doi.org/10.1021/acs.energyfuels.1c01225
Energy Fuels 2021, 35, 11525−11532